Electrically tunable Yb-doped fiber laser based on a liquid crystal photonic bandgap fiber device

Olausson, Christina Bjarnal Thulin; Scolari, Lara; Wei, Lei; Noordegraaf, Danny; Weirich, Johannes; Alkeskjold, Thomas Tanggaard; Hansen, Kim P.; Bjarklev, Anders Overgaard

Published in:
Optics Express

Link to article, DOI:
10.1364/OE.18.008229

Publication date:
2010

Document Version
Publisher's PDF, also known as Version of record

Electrically tunable Yb-doped fiber laser based on a liquid crystal photonic bandgap fiber device

Christina B. Olausson[1,2*], Lara Scolari[2], Lei Wei[2], Danny Noordegraaf[1,2], Johannes Weirich[2], Thomas T. Alkeskjold[1], Kim P. Hansen[1], and Anders Bjarklev[2]

[1]*NKT Photonics A/S, Blokken 84, DK-3460 Birkerød, Denmark*
[2]*DTU Fotonik, Department of Photonic Engineering, Technical University of Denmark, Ørsteds Plads 343, DK-2800 Kgs. Lyngby, Denmark*
**cbo@nktphotonics.com*

Abstract: We demonstrate electrical tunability of a fiber laser using a liquid crystal photonic bandgap fiber. Tuning of the laser is achieved by combining the wavelength filtering effect of a tunable liquid crystal photonic bandgap fiber device with an ytterbium-doped photonic crystal fiber. We fabricate an all-spliced laser cavity based on the liquid crystal photonic bandgap fiber mounted on a silicon assembly, a pump/signal combiner with single-mode signal feed-through and an ytterbium-doped photonic crystal fiber. The laser cavity produces a single-mode output and is tuned in the range 1040-1065 nm by applying an electric field to the silicon assembly.

OCIS codes: (060.5295) Photonic crystal fibers; (230.3720) Liquid-crystal devices; (060.3510) Lasers, fiber.

References and links

1. P. St. J. Russell, "Photonic Crystal Fibers," Science **299**(5605), 358–362 (2003).
2. N. M. Litchinitser, S. C. Dunn, P. E. Steinvurzel, B. J. Eggleton, T. P. White, R. C. McPhedran, and C. M. de Sterke, "Application of an ARROW model for designing tunable photonic devices," Opt. Express **12**(8), 1540–1550 (2004), http://www.opticsinfobase.org/abstract.cfm?URI=oe-12-8-1540.
3. S. Gauza, C. H. Wen, S. T. Wu, N. Janarthanan, and C. S. Hsu, "Super high birefringence isothiocyanato biphenyl-bistolane liquid crystals," Jpn. J. Appl. Phys. **43**(No. 11A), 7634–7638 (2004).
4. S. T. Wu, Q. T. Zhang, and S. Marder, "High dielectric dopants for low voltage liquid crystal operation," Jpn. J. Appl. Phys. **37**(Part 2, No. 10B), L1254–L1256 (1998).
5. B. J. Eggleton, C. Kerbage, P. S. Westbrook, R. S. Windeler, and A. Hale, "Microstructured optical fiber devices," Opt. Express **9**(13), 698–713 (2001), http://www.opticsinfobase.org/oe/abstract.cfm?URI=oe-9-13-698.
6. C. Kerbage, R. S. Windeler, B. J. Eggleton, P. Mach, M. Dolinski, and J. A. Rogers, "Tunable devices based on dynamic positioning of micro-fluids in micro-structured optical fiber," Opt. Commun. **204**(1-6), 179–184 (2002).
7. R. T. Bise, R. S. Windeler, K. S. Kranz, C. Kerbage, B. J. Eggleton, and D. J. Trevor, "Tunable photonic band gap fiber," in *Optical Fiber Communication Conference and Exhibit, 2002. OFC 2002*, pp. 466–468.
8. T. T. Larsen, A. Bjarklev, D. S. Hermann, and J. Broeng, "Optical devices based on liquid crystal photonic bandgap fibres," Opt. Express **11**(20), 2589–2596 (2003), http://www.opticsinfobase.org/oe/abstract.cfm?URI=oe-11-20-2589.
9. M. W. Haakestad, T. T. Alkeskjold, M. D. Nielsen, L. Scolari, J. Riishede, H. E. Engan, and A. Bjarklev, "Electrically tunable photonic bandgap guidance in a liquid-crystal-filled photonic crystal fiber," IEEE Photon. Technol. Lett. **17**(4), 819–821 (2005).
10. L. Scolari, T. T. Alkeskjold, J. Riishede, A. Bjarklev, D. Hermann, A. Anawati, M. Nielsen, and P. Bassi, "Continuously tunable devices based on electrical control of dual-frequency liquid crystal filled photonic bandgap fibers," Opt. Express **13**(19), 7483–7496 (2005), http://www.opticsinfobase.org/oe/abstract.cfm?URI=oe-13-19-7483.
11. F. Du, Y. Q. Lu, and S. T. Wu, "Electrically tunable liquid-crystal photonic crystal fiber," Appl. Phys. Lett. **85**(12), 2181–2183 (2004).
12. T. T. Alkeskjold, J. Lægsgaard, A. Bjarklev, D. Hermann, A. Anawati, J. Broeng, J. Li, and S. T. Wu, "All-optical modulation in dye-doped nematic liquid crystal photonic bandgap fibers," Opt. Express **12**(24), 5857–5871 (2004), http://www.opticsinfobase.org/oe/abstract.cfm?URI=oe-12-24-5857.
13. L. Scolari, T. T. Alkeskjold, and A. Bjarklev, "Tunable Gaussian filter based on tapered liquid crystal photonic bandgap fibre," Electron. Lett. **42**(22), 1270–1271 (2006).

#121794 - $15.00 USD Received 21 Dec 2009; revised 11 Mar 2010; accepted 16 Mar 2010; published 5 Apr 2010

14. D. Noordegraaf, L. Scolari, J. Lægsgaard, L. Rindorf, and T. T. Alkeskjold, "Electrically and mechanically induced long period gratings in liquid crystal photonic bandgap fibers," Opt. Express **15**(13), 7901–7912 (2007), http://www.opticsinfobase.org/oe/abstract.cfm?URI=oe-15-13-7901.
15. M. N. Petersen, L. Scolari, T. Tokle, T. T. Alkeskjold, S. Gauza, S.-T. Wu, and A. Bjarklev, "Noise filtering in a multi-channel system using a tunable liquid crystal photonic bandgap fiber," Opt. Express **16**(24), 20067–20072 (2008), http://www.opticsinfobase.org/oe/abstract.cfm?URI=oe-16-24-20067.
16. T. R. Woliński, S. Ertman, A. Czapla, P. Lesiak, K. Nowecka, A. W. Domanski, E. Nowinowski-Kruszelnicki, R. Dabrowski, and J. Wojcik, "Polarization effects in photonic liquid crystal fibers," Meas. Sci. Technol. **18**(10), 3061–3069 (2007).
17. T. R. Woliński, A. Czapla, S. Ertman, M. Tefelska, A. W. Domanski, E. Nowinowski-Kruszelnicki, and R. Dabrowski, "Tunable highly birefringent solid-core photonic liquid crystal fibers," Opt. Quantum Electron. **39**(12-13), 1021–1032 (2007).
18. D. C. Zografopoulos, E. E. Kriezis, and T. D. Tsiboukis, "Tunable highly birefringent bandgap-guiding liquid crystal microstructured fibers," J. Lightwave Technol. **24**(9), 3427–3432 (2006).
19. L. Wei, W. Xue, Y. Chen, T. T. Alkeskjold, and A. Bjarklev, "Optically fed microwave true-time delay based on a compact liquid-crystal photonic-bandgap-fiber device," Opt. Lett. **34**(18), 2757–2759 (2009).
20. V. Pureur, L. Bigot, G. Bouwmans, Y. Quiquempois, M. Douay, and Y. Jaouen, "Ytterbium-doped solid core photonic bandgap fiber for laser operation around 980 nm," Appl. Phys. Lett. **92**(6), 061113 (2008).
21. A. Shirakawa, H. Maruyama, K. Ueda, C. B. Olausson, J. K. Lyngsø, and J. Broeng, "High-power Yb-doped photonic bandgap fiber amplifier at 1150-1200 nm," Opt. Express **17**(2), 447–454 (2009), http://www.opticsinfobase.org/oe/abstract.cfm?URI=oe-17-2-447.
22. L. Wei, E. Khomtchenko, T. T. Alkeskjold, and A. Bjarklev, "Photolithography of thick photoresist coating for electrically controlled liquid crystal photonic bandgap fiber devices," Electron. Lett. **45**(6), 326–327 (2009).
23. L. Wei, T. T. Alkeskjold, and A. Bjarklev, "Compact design of an electrically tunable and rotatable polarizer based on a liquid crystal photonic bandgap fiber," IEEE Photon. Technol. Lett. **21**(21), 1633–1635 (2009).
24. D. Noordegraaf, M. D. Nielsen, P. M. Skovgaard, S. Agger, K. P. Hansen, J. Broeng, C. Jakobsen, H. R. Simonsen, and J. Lægsgaard, "Pump Combiner for Air-Clad Fiber with PM Single-Mode Signal Feed-through," in *Conference on Lasers and Electro-Optics/International Quantum Electronics Conference*, OSA Technical Digest (CD) (Optical Society of America, 2009), paper CThGG6.
25. J. Weirich, J. Laegsgaard, L. Scolari, L. Wei, T. T. Alkeskjold, and A. Bjarklev, "Biased liquid crystal infiltrated photonic bandgap fiber," Opt. Express **17**(6), 4442–4453 (2009), http://www.opticsinfobase.org/oe/abstract.cfm?URI=oe-17-6-4442.
26. J. Weirich, J. Laegsgaard, L. Wei, T. T. Alkeskjold, T. X. Wu, S. Wu, and A. Bjarklev, "Liquid crystal parameter analysis for tunable photonic bandgap fiber devices," Opt. Express **18**(5), 4074–4087 (2010), http://www.opticsinfobase.org/oe/abstract.cfm?URI=oe-18-5-4074.

1. Introduction

A typical photonic crystal fiber (PCF) obtains its waveguide properties from an arrangement of airholes in a silica cladding surrounding a solid core [1]. The airholes lower the average refractive index of the cladding, allowing the fiber to guide by modified total internal reflection (TIR). Furthermore, a microstructured cladding can allow for waveguidance by the photonic bandgap (PBG) effect where light is confined within a low-index core by means of coherent reflections from the surrounding periodic structure [2]. The design structure of PCFs offers the unique possibility of infiltrating the airholes of a TIR guiding PCF with a high-index liquid material and thereby give rise to guidance by the photonic bandgap (PBG) effect. Among high-index liquid materials, liquid crystals (LCs) exhibit large electro-optic and thermo-optic effects due to high birefringence ($\Delta n \sim 0.8$) [3] and large dielectric anisotropy ($\Delta\varepsilon \sim 70$) [4]. These effects can be exploited to control the bandgap properties of the fiber in order to fabricate all-in-fiber devices employing either thermal, electrical or optical tunability [5–7]. A number of such liquid crystal photonic bandgap (LCPBG) devices have been demonstrated [8–19].

Combining the wavelength filtering effect of PBG confinement with an ytterbium-doped core has previously been used in solid-core PBG fiber lasers and amplifiers. The bandgap efficiently suppresses the amplified spontaneous emission (ASE) at the conventional ytterbium gain wavelengths around 1030nm and enables both short [20] and long wavelength operation [21]. In this work we merge the PBG fiber laser concept with the tunability offered by LCs to create an all-spliced fiber laser with electrical tunability in the range 1040-1065 nm. The presence of a bandgap in the laser cavity will inhibit lasing at certain wavelengths, thus by applying an electric field to an intra-cavity LCPBG fiber the bandgap position can be shifted, resulting in laser tunability. This is to our knowledge the first LC based electrically

#121794 - $15.00 USD Received 21 Dec 2009; revised 11 Mar 2010; accepted 16 Mar 2010; published 5 Apr 2010

tunable fiber laser. The device holds potential as a low cost tunable seed source for ytterbium fiber amplifiers.

2. Liquid crystal photonic bandgap fiber

The LC used in the present work is a dual-frequency LC (MDA-00-3969, Merck). Polarization microscopy studies of this LC show that it is aligned in a splay configuration with an angle of 45° at the boundary surface [10]. At room temperature the LC is in the nematic phase where the molecules possess orientational order but not positional order. When an electric field is applied to the LC it exerts a torque on the LC director, which is rotated parallel or perpendicular to the field direction, depending on the sign of the dielectric anisotropy. In general, dual-frequency LCs behave differently depending on the frequency of the applied electric field. For the present LC the dielectric anisotropy is positive if the electric field is below 15 kHz and negative if the electric field is above this value, hence allowing for electric control of the spectral position of the bandgap towards both shorter and longer wavelengths in the same device. A frequency of 1 kHz is used in the experiment since we wish to operate the laser close to the short wavelength edge of the bandgap and tune the bandgap edge towards longer wavelengths. Figure 1(a) shows an enlargement of a single capillary filled with LC. The blue arrows show the orientation of the LC director, while the black arrows show the direction along which the LC tends to reorient when a 1 kHz field is applied. The LC has wavelength dependent ordinary and extraordinary refractive indices of n_o = 1.4978 and n_e = 1.7192 respectively, at T = 20°C and λ = 589.2 nm. Previous studies of this LC [10] show that the response time is in the ms range. The rise time is about 3 ms for a voltage of 100 Vrms at 1 kHz, while the decay time is 12 ms.

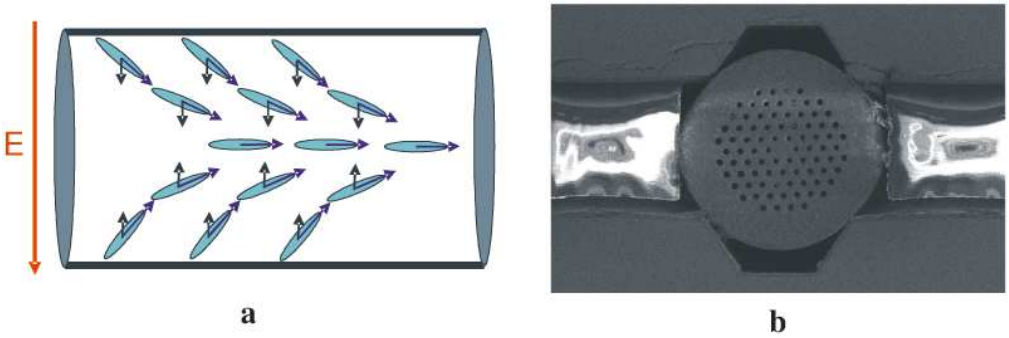

Fig. 1. (a) Illustration of an enlarged capillary filled with LC. The blue arrows show the orientation of the LC director, while the black arrows show the direction along which the LC tends to reorient when a 1 kHz field is applied. (b) SEM image of the LMA 13 fiber placed in the silicon assembly.

The fiber used in the experiment is a large-mode-area PCF (LMA-13) with a hole diameter of 4.3 μm, an inter-hole distance of 8.5 μm and a cladding diameter of 125 μm. The 13 μm core is surrounded by five rings of airholes arranged in a triangular lattice. The LC is infiltrated by capillary forces without application of external forces in order to minimize deformations of the LC alignment. The LC infiltrated section of the fiber is 13 mm long. A SEM image of the fiber end facet is shown in Fig. 1(b). The surrounding structure is the silicon assembly.

#121794 - $15.00 USD Received 21 Dec 2009; revised 11 Mar 2010; accepted 16 Mar 2010; published 5 Apr 2010

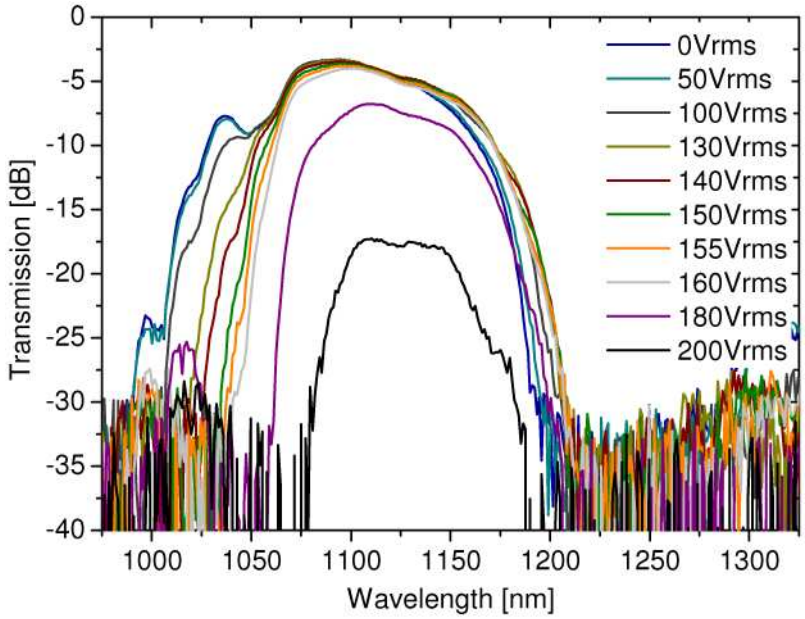

Fig. 2. Transmission spectrum of the LCPBG device as a function of applied voltage. The frequency of the applied electric field is 1 kHz.

3. Electrically controlled LCPBG fiber device

When the LCPBG fiber is placed between electrodes the spectral position of the bandgaps in the LC filled section of the fiber can be electrically tuned. Applying a 1 kHz sine wave in bipolar mode across the fiber causes the refractive index in the transverse plane to increase thus shifting the bandgap towards longer wavelengths as shown in Fig. 2. The short wavelength bandgap edge is situated around the typical ytterbium gain wavelengths 1030-1080 nm, which makes the device well suited for an ytterbium-doped fiber laser. This position of the short wavelength edge of the bandgap allows for filtering of short wavelength ASE which is the main limitation in ytterbium-doped fiber lasers. When the voltage is increased, the bandgap edge and the laser wavelength will move towards longer wavelengths. The main loss mechanism is coupling loss between the TIR mode of the unfilled fiber and the PBG mode of the filled fiber. At voltages above 160 V_{rms} the transmission becomes lossy as the PBG mode becomes less confined in the silica core.

Packaging of the LCPBG fiber device is critical in order to achieve a compact and easy-to-use device. The LC infiltrated section of the LMA-13 is placed in a v-groove fabricated on silicon substrate and the end facet is placed just outside the chip in order to enable coupling of light as shown in Fig. 3. A pair of Au electrodes is deposited on the sidewalls of the groove, and the electrode patterning is achieved by using thick photoresist coating and two-step exposure [22]. The electrodes are electrically isolated from the silicon substrate by a 2 μm SiO_2 layer and a thin titanium layer is used as an adhesion layer between the electrodes and the isolation layer. A top lid containing a v-groove with the other pair of electrodes is placed on top of the fiber, forming two sets of electrodes, which fix the fiber at four orthogonal corners relative to the fiber core. In order to ensure a good contact between the LCPBG fiber and the electrodes, SU-8 fiber fixing structures are built up on the electrodes [23]. The height of each SU-8 structure is 84 μm and the distance between two neighboring structures is 126 μm, taking the small variation of the fiber outer diameter into account. The assembly is sealed with epoxy.

#121794 - $15.00 USD Received 21 Dec 2009; revised 11 Mar 2010; accepted 16 Mar 2010; published 5 Apr 2010

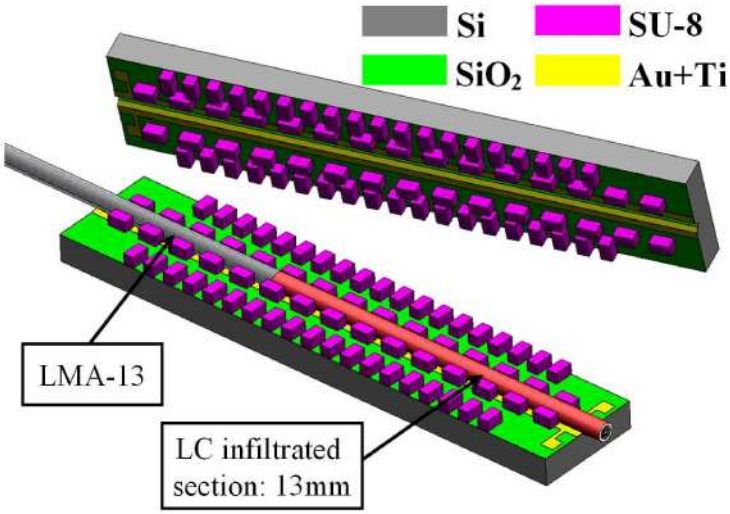

Fig. 3. Illustration of the silicon assembly for the LCPBG device.

4. All-spliced laser cavity with single-mode combiner

The all-spliced fiber assembly is comprised of the LCPBG fiber device, an ytterbium-doped airclad PCF, a pump diode and a 6+1:1 pump/signal combiner for airclad fibers with polarization-maintaining (PM) single-mode signal feed-through. The combiner is designed for 0.15 NA pump diodes, and in order to utilize the high NA supported by airclad fibers, it features a special taper element [24].

The LCPBG fiber device is spliced to the single-mode signal feed-through of the combiner while the delivery fiber of the combiner is spliced to a PM ytterbium-doped airclad PCF. The laser cavity is formed by a lens and silver mirror after the LCPBG fiber device and the cleaved end facet of the ytterbium-doped PCF. The ytterbium-doped PCF has a pump cladding diameter of 105 μm, a mode field diameter of 12 μm and is cleaved at a 0° angle to allow for approximately 4% reflectivity. With a pump absorption of ~3 dB/m and a length of 4 m it is optimized for 976 nm pumping. The residual pump is filtered by a long wave pass filter at the output of the laser cavity while the laser signal spectrum is recorded by an optical spectrum analyzer (OSA). An illustration of the all-spliced laser cavity is shown in Fig. 4. Besides ease-of-use and compactness, an additional incentive to use the pump/signal combiner rather than pumping through a dichroic mirror is that cladding pumping directly through the LC filled section might affect the behavior of the LC.

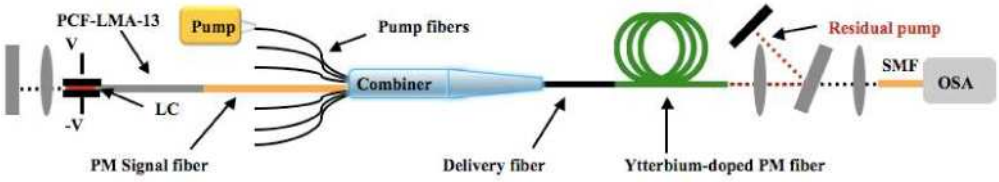

Fig. 4. All-spliced laser cavity setup from the left: cavity mirror, LCPBG fiber mounted on a silicon assembly, pump/signal combiner with single-mode signal feed-through, ytterbium-doped PCF, long wave pass filter, and OSA.

5. Tunability of the LCPBG fiber laser

Bandgap tunability of the all-spliced fiber assembly is investigated by applying a voltage of up to 200 V_{rms} to the LCPBG device. Figure 5 shows the transmission spectra of the assembly for different voltage settings. Below 100 V_{rms} the bandgap is unchanged, from 100 to 160 V_{rms} the short wavelength edge of the bandgap is shifted towards longer wavelengths by

#121794 - $15.00 USD Received 21 Dec 2009; revised 11 Mar 2010; accepted 16 Mar 2010; published 5 Apr 2010

approximately 25 nm. Above 160 V_{rms} the losses in the bandgap increase dramatically. The total loss in the cavity due to the LC insertion, the combiner and splices is measured to approximately 6 dB and is mainly due to mode-matching errors at the interface between the LMA fiber and the PM signal feed-through fiber and due to coupling losses between the TIR mode and the PBG mode of the LMA fiber. Considering the high losses in the bandgap above 160 V_{rms}, the laser cavity is only expected to be tunable at lower voltage setting. A near field image of the single-mode output from the laser cavity is shown Fig. 6.

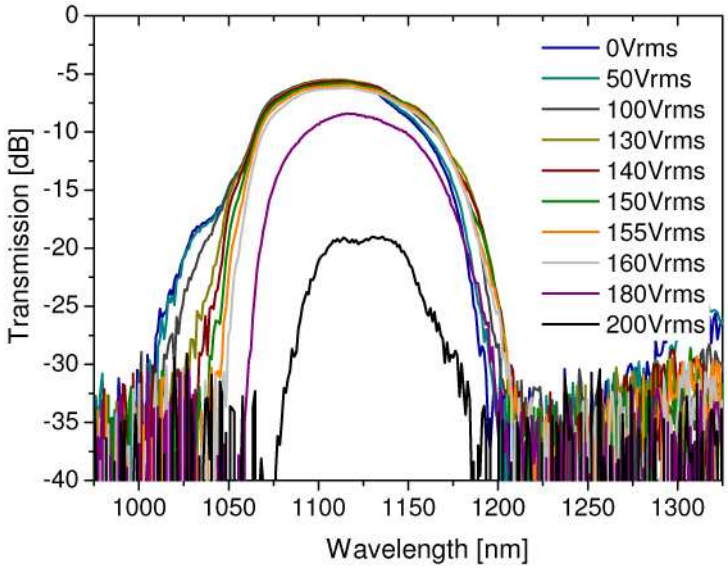

Fig. 5. Transmission spectrum of the all-spliced fiber assembly. The short wavelength bandgap edge is shifted towards longer wavelengths when a voltage is applied. Above 160 Vrms the losses in the bandgap become high.

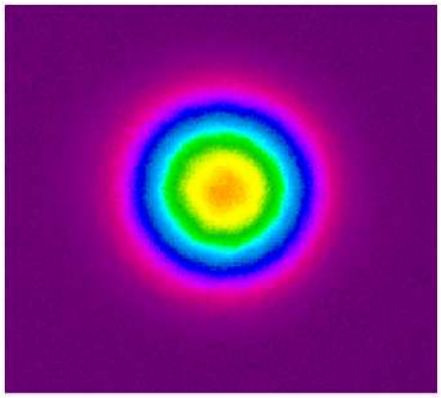

Fig. 6. Near field image of the single-mode output from the laser cavity.

#121794 - $15.00 USD Received 21 Dec 2009; revised 11 Mar 2010; accepted 16 Mar 2010; published 5 Apr 2010

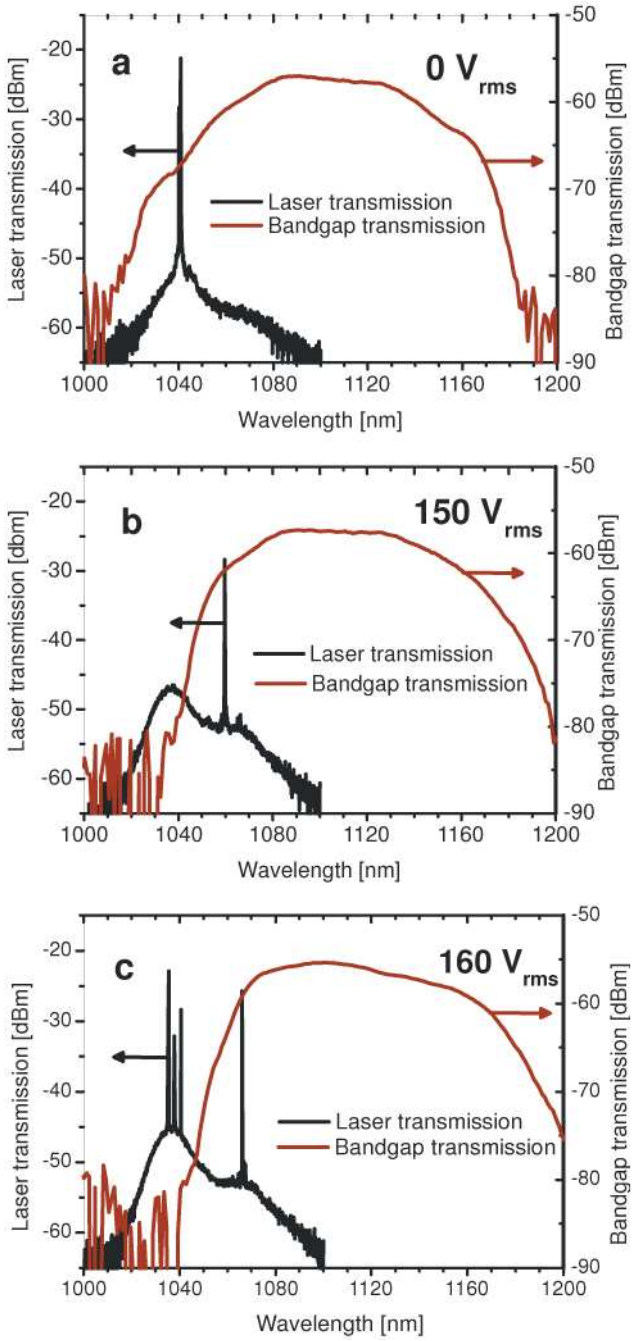

Fig. 7. Laser transmission spectra compared to bandgap transmission spectra for two different voltage settings, (a) 0 V_{rms}, (b) 150 V_{rms}, and (c) 160 V_{rms}. The plots show how the cavity is lasing close to the short wavelength bandgap edge. Parasitic lasing outside the bandgap will limit the power and tunability of the laser at high voltages.

In PBG fiber lasers, lasing will occur at the wavelengths that experience the least loss due to the bandgap combined with the highest gain due to their emission cross section. These wavelengths are close to the short wavelength edge of the bandgap. Fiber lasers based on active PBG fibers typically have distributed spectral filtering along the whole length of the

#121794 - $15.00 USD Received 21 Dec 2009; revised 11 Mar 2010; accepted 16 Mar 2010; published 5 Apr 2010

fiber in order to reduce ASE, whereas in the LCPBG device the LC infiltrated section is only 13 mm long. Hence, ASE will inevitably build up in the ytterbium-doped fiber, resulting in parasitic lasing which will limit the tunability and power scalability of the LCPBG fiber laser. Figure 7(a-c) shows the laser transmission spectra compared to the bandgap transmission spectra for three different voltage setting, 0 V_{rms}, 150 V_{rms}, and 160 V_{rms}. For low voltages the ASE peak is well inside the bandgap and therefore tuning of the bandgap edge does not affect the lasing wavelength significantly. For higher voltages the ASE peak is outside the bandgap, while the laser wavelength is tuned inside the bandgap. For voltages of 160 V_{rms} and higher, the loss inside the bandgap becomes too high leading to parasitic lasing outside the bandgap. Had a frequency above 15 kHz been applied instead, the bandgap edge would have moved towards shorter wavelengths, the ASE peak around 1040 nm would have remained inside the bandgap and tuning of the laser would have been impossible.

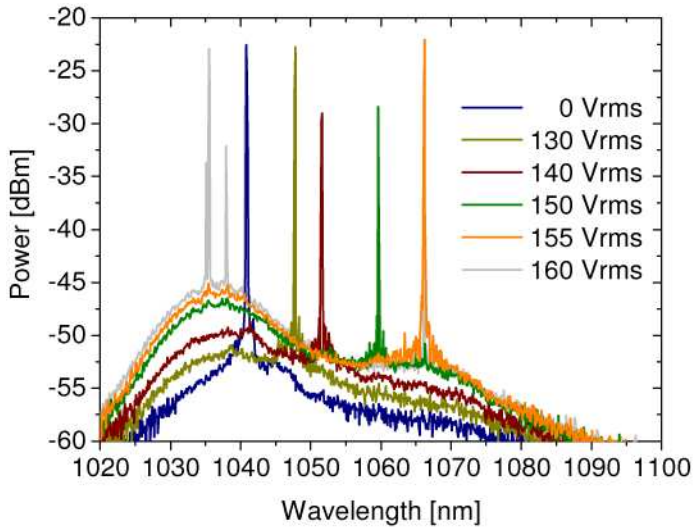

Fig. 8. The laser wavelength is shifted towards longer wavelengths. At 160 V_{rms} parasitic lasing sets in at shorter wavelengths. A total shift of 25 nm is observed.

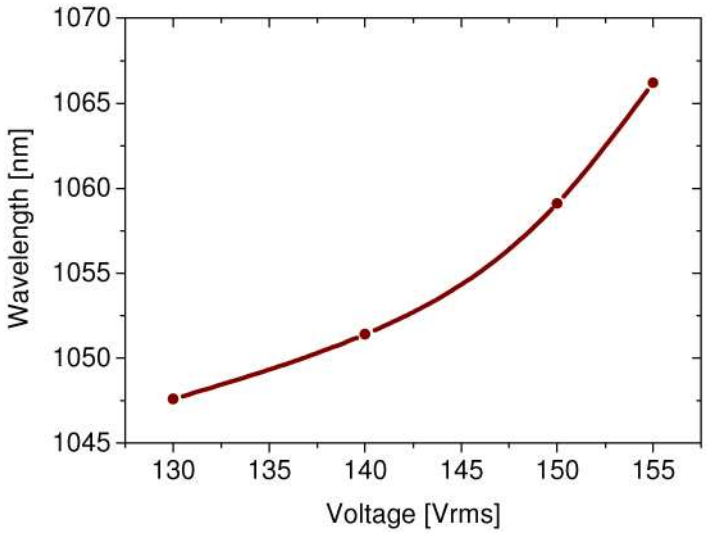

Fig. 9. The laser wavelength plotted as a function of applied voltage. Tuning starts above 130 V_{rms}. The wavelength is constant at 1040 nm below 130 V_{rms}.

#121794 - $15.00 USD Received 21 Dec 2009; revised 11 Mar 2010; accepted 16 Mar 2010; published 5 Apr 2010

Figure 8 shows the narrow laser spectra of the cavity for different voltage settings. The laser wavelength is shifted towards longer wavelengths by approximately 25 nm. The pump power is increased between each measurement to keep lasing just above threshold and as a consequence ASE builds up in the cavity when the pump power is increased. The ASE build-up causes parasitic lasing at shorter wavelengths for voltages around 160 Vrms and higher, eventually limiting both the power and the tuning range of the laser. The laser wavelength is plotted as a function of applied voltage in Fig. 9. The wavelength is constant at 1040 nm below 130 Vrms and tunable up to 1065 nm at 155 Vrms.

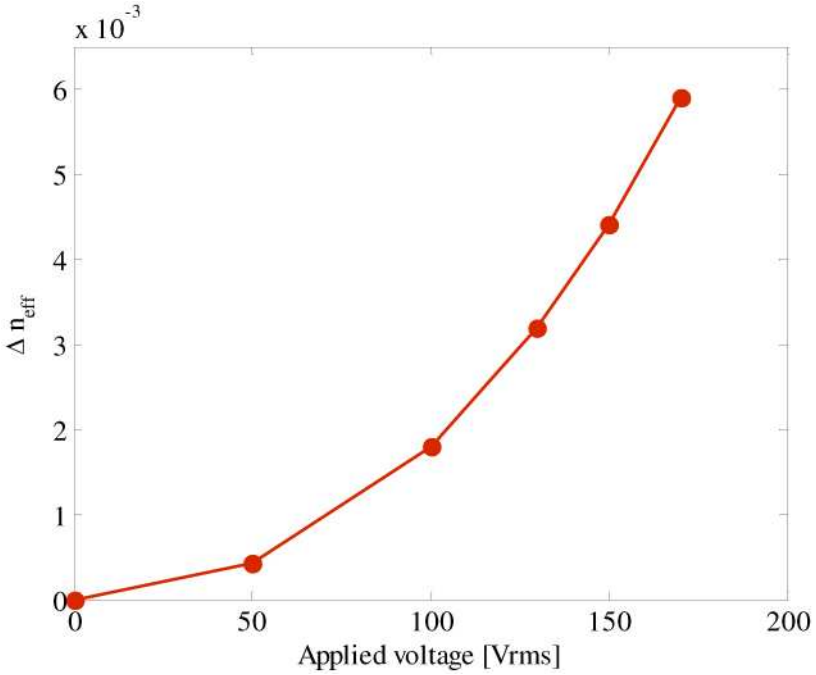

Fig. 10. Simulated change of effective index of the capillary mode responsible for the short wavelength bandgap edge. The dependence of the effective index shift on the applied external field is found to be quadratic.

We have shown that the lasing wavelength is determined by the position of the bandgap edge of the LCPBG device, which in turn is influenced by the refractive index structure in the LC. Since the LC is splay aligned the modes in the capillaries see a spatially varying anisotropic refractive index structure which changed when an external electric field is applied. The change in effective index is determined by the orientation of the LCs and this reorientation depends quadratically on the applied electric field [25,26]. Figure 10 shows the simulated change of effective index of the capillary mode responsible for the short wavelength bandgap edge. Also here we find a quadratic dependence of the effective index shift on the applied external electric field. Thus, as expected the tuning in Fig. 9 is not linear.

The laser cavity produced an output of ~30 mW with the efficiency of the laser strongly limited by losses in the cavity. With optimization of cavity optics, fiber cleave angles, LC device, and mode-matching between fibers, losses can be reduced and potentially allow for the production of an easily tunable, single-mode output signal, which can be used to seed a fiber amplifier. The present cavity yields up to 25 dB of ASE suppression, however an improved cavity with reflectors in both ends is expected to improve the ASE suppression significantly. The polarization-maintaining properties of the device are expected to be good.

#121794 - $15.00 USD Received 21 Dec 2009; revised 11 Mar 2010; accepted 16 Mar 2010; published 5 Apr 2010

6. Conclusion

We have fabricated an all-spliced fiber laser cavity with a single-mode output, which is electrically tunable from 1040 nm to 1065 nm. The device is based on an LCPBG fiber mounted on a silicon assembly, a pump/signal combiner and an ytterbium-doped PCF. The LCPBG fiber device induces a bandgap in the cavity, which is tuned by an electric field and used to shift the laser wavelength by 25 nm. This is to our knowledge the first LC based electrically tunable fiber laser. With improvements to the system, the device holds potential as a low cost, compact and easy-to-use tunable seed source for fiber amplifiers. Improvements can by obtained by reducing the cavity losses or by reducing the number of components and interfaces in the cavity, e.g. by infiltrating LC directly in an ytterbium-doped PCF.

#121794 - $15.00 USD Received 21 Dec 2009; revised 11 Mar 2010; accepted 16 Mar 2010; published 5 Apr 2010